3336 *Biochemistry* **2010,** *49,* 3336–3342
DOI: 10.1021/bi100176a

BIOCHEMISTRY
including biophysical chemistry & molecular biology
Article

Circular Dichroism and UV Resonance Raman Study of the Impact of Alcohols on the Gibbs Free Energy Landscape of an α-Helical Peptide†

Kan Xiong and Sanford A. Asher*

Department of Chemistry, University of Pittsburgh, Pittsburgh, Pennsylvania 15260

Received February 4, 2010; Revised Manuscript Received March 11, 2010

ABSTRACT: We used CD and UV resonance Raman spectroscopy to study the impact of alcohols on the conformational equilibria and relative Gibbs free energy landscapes along the Ramachandran Ψ-coordinate of a mainly poly-Ala peptide, AP with an AAAAA(AAARA)$_3$A sequence. 2,2,2-Trifluoroethanol (TFE) most stabilizes the α-helix-like conformations, followed by ethanol, methanol, and pure water. The π-bulge conformation is stabilized more than the α-helix, while the 3_{10}-helix is destabilized due to the alcohol-increased hydrophobicity. Turns are also stabilized by alcohols. We also found that while TFE induces more α-helices, it favors multiple, shorter helix segments.

Protein (peptide) folding depends on both its primary sequence and its solvent environment. Addition of alcohol to an aqueous solution changes the hydration of the protein (peptide). The resulting conformational changes can be used as a valuable tool for probing protein (peptide)−water interactions (*1*−*7*). It is important to realize that despite intensive investigations over the years, the mechanism(s) by which alcohols perturb protein conformation is still poorly understood (*8*−*18*).

In this work, we used CD and UV resonance Raman (UVRR) spectroscopy to study the impact of alcohols on the conformational equilibria and relative Gibbs free energy landscapes along the Ramanchandran Ψ-coordinate of a mainly poly-Ala peptide, AP with an AAAAA(AAARA)$_3$A sequence. We find that the α-helix and π-bulge conformations are most stabilized by 2,2,2-trifluoroethanol (TFE), followed by ethanol, methanol, and pure water. Turn conformations are also stabilized. However, 3_{10}-helices are destabilized. We also find that TFE induces an increased abundance of α-helices. However, the average α-helix length is decreased.

EXPERIMENTAL PROCEDURES

The 21-residue peptide AP with an AAAAA(AAARA)$_3$A sequence was purchased from AnaSpec Inc. (>95% purity). Absolute methanol was purchased from J. T. Baker. Absolute ethanol was purchased from Pharmco. 2,2,2-Trifluoroethanol (TFE, 99.8% purity) was purchased from Acros. The pH 7 solution samples contain 1 mg/mL AP and 0.05 M $NaClO_4$.

The CD spectra were recorded by using a Jasco-715 spectropolarimeter, by using a 0.02 cm path length cuvette. We co-added five individual CD spectra.

The UV resonance Raman (UVRR) apparatus was described in detail by Bykov et al. (*19*). Briefly, 204 nm UV light (1 mW average power, 100 μm diameter spot) was obtained by mixing the third harmonic with the fundamental (816 nm wavelength, 1 kHz repetition rate, 0.6 W average power, 25−40 ns pulse width) of a tunable Ti:Sapphire laser system from Photonics Industries. The sample was circulated in a free surface, temperature-controlled stream. A 180° sampling backscattering geometry was used. The collected light was dispersed by a double monochromator onto a back-thinned CCD camera (Princeton Instruments Spec 10 System, 1.5 cm^{-1} resolution with a 100 μm slit width). We used 5 min accumulation times, and four accumulations were co-added. The 732 and 1379.5 cm^{-1} bands of Teflon were utilized to calibrate the frequencies. The frequencies are reproducible to less than 1 cm^{-1}. Raman spectra were normalized to the peak height of the 932 cm^{-1} ClO_4^- band. No Raman saturation occurs at these low excitation powers.

RESULTS

CD Measurements. Figure 1 shows the temperature dependence of the CD spectra of AP in pure water. The low-temperature CD spectra show two troughs at 222 and 206 nm that are characteristic of α-helix conformations (*20*). As the temperature increases, the ellipticity at 222 nm, θ_{222}, becomes less negative, indicating α-helix melting. The isosbestic point at 202 nm indicates that the melting behavior appears spectroscopically as a "two-state" process. Previous work by our group demonstrated that the AP α-helix conformation melts to a dominantly PPII-like conformation (*21*).

Panels a and b of Figure 2 show the temperature dependence of the mean residue ellipticity at 222 nm, θ_{222}, of AP in pure water and in the presence of different alcohols. Alcohols increase the α-helix content. At 20 °C and 25% alcohol by volume, TFE most stabilizes the α-helix, followed closely by ethanol and then methanol, consistent with previous studies (*8*, *12*, *18*). At 50% (v/v) alcohol, ethanol is the most α-helix-stabilizing, followed by TFE and then methanol. As the alcohol concentration increases from 25 to 50%, θ_{222} decreases in methanol and ethanol but changes little in TFE (Figure 2c). Previous studies also showed that TFE does not appear in CD measurements to induce additional α-helix concentrations above 25% (v/v) (*11*).

UVRR Measurements. The 204 nm UV Raman spectra (UVRS) of AP in pure water (Figure 3) show mainly the amide

†The work was supported by National Institutes of Health Grants GM8RO1EB002053 and 1RO1EB009089.
*To whom correspondence should be addressed. Phone: (412) 624-8570. Fax: (412) 624-0588. E-mail: asher@pitt.edu.

 Published on Web 03/12/2010

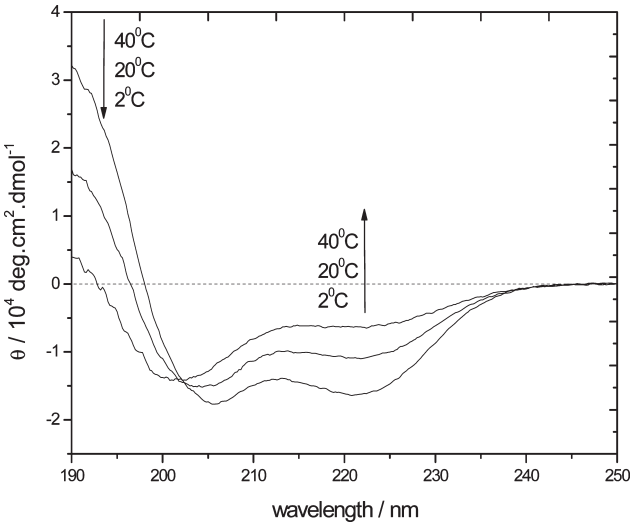

FIGURE 1: Temperature dependence of the CD spectra of 1 mg/mL AP in pure water.

RR bands. In contrast, the 204 nm UVRS of AP in 50% methanol (Figure 3) show methanol Raman bands which we numerically removed in the Figure 4 UVRS. The resulting spectra show the temperature dependence of the 204 nm UVRS of AP in 50% methanol. As the temperature increases, the AmI band upshifts from 1652 to 1658 cm^{-1} while the AmII band downshifts from 1556 to 1552 cm^{-1} (*22*). Previous work (*23*) indicates that water hydrogen bonding to the peptide bond (PB) C═O site increases the C═O bond length and, thus, downshifts the AmI band, while water hydrogen bonding to the PB N−H site upshifts the AmII band. The AmI (AmII) band in pure water (Figure 4) is upshifted (downshifted) relative to that in 50% methanol, indicating less C═O (N−H) hydrogen bonding in an alcohol solution (*23*). The C_α−H doublet (~1372 and ~1393 cm^{-1}) frequency does not shift as the temperature increases but its intensity increases.

The C_α−H doublet intensity only slightly increases from 2 to 20 °C, indicating little α-helix melting (*24*). Significant intensity changes observed from 20 to 40 °C indicate extensive α-helix melting. The $AmIII_3$ band downshifts from ~1264 cm^{-1} at 2 °C to ~1259 cm^{-1} at 40 °C while its intensity increases (*22*). UVRS of AP in other alcohols (not shown) show very similar α-helix melting behaviors.

To calculate the α-helical fractions, we subtracted appropriate amounts of the temperature-dependent PPII-like conformation basis spectra (*22*) from the measured and digitally smoothed UVRS of AP to minimize the C_α−H region intensity in the difference spectra. The basis spectral intensities subtracted are directly proportional to the concentrations of the PPII-like conformation at each temperature. The resulting difference spectra appear to be mainly α-helix-like. Figure 5 shows UVRR-calculated fractions of α-helix-like conformation of AP in pure water and in 50% (v/v) alcohol. The α-helix-like conformations are dramatically stabilized in alcohol and melt little as the temperature increases. TFE stabilizes the α-helix-like conformations the most, followed by ethanol, and then methanol, as previously observed (*8*, *12*, *18*). The α-helix-like conformation melting curves in ethanol and in methanol are essentially identical. These conclusions obviously differ from the CD conclusions.

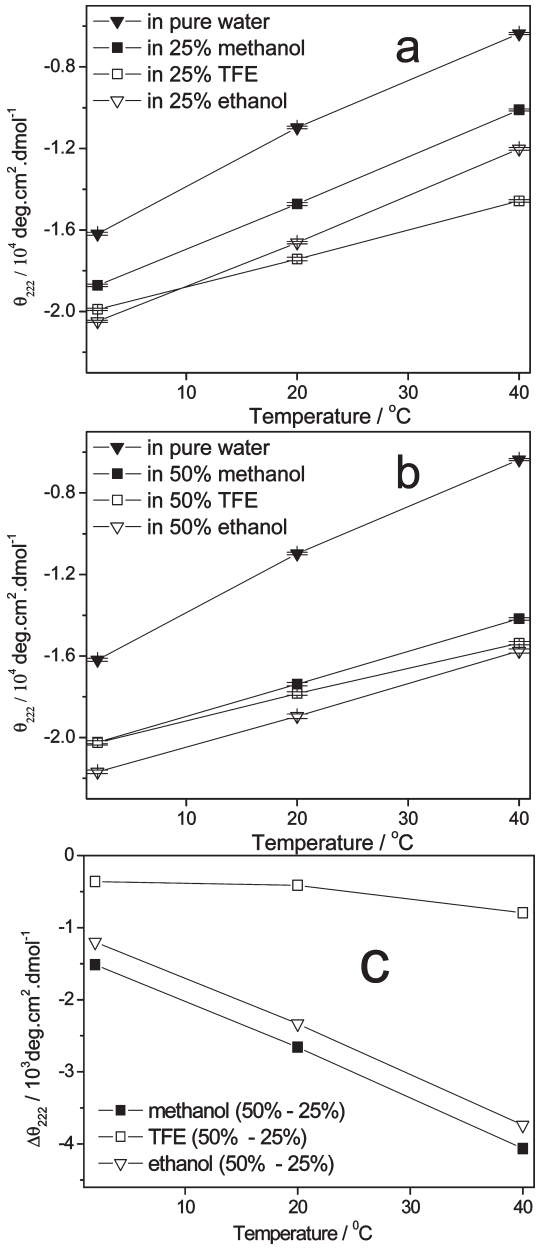

FIGURE 2: (a) θ_{222} of AP in 25% (v/v) alcohol. (b) θ_{222} of AP in 50% (v/v) alcohol. (c) $\Delta\theta_{222}$ (θ_{222} in 50% alcohol minus θ_{222} in 25% alcohol).

Figure 6 shows the calculated α-helix-like spectra of AP in pure water and in 50% (v/v) methanol. The $AmIII_3$ band in pure water shows a peak at ~1258 cm^{-1} with a shoulder at ~1280 cm^{-1} and another shoulder at ~1240 cm^{-1}. Previous work showed that an $AmIII_3$ band at ~1258 cm^{-1} indicates the pure α-helical conformation, a band at ~1280 cm^{-1} indicates a π-helix (bulge), and a band at ~1240 cm^{-1} indicates a 3_{10}-helix (*25*). The $AmIII_3$ band in pure water narrows at higher temperatures as previously observed (*26*, *27*), indicating decreased concentrations of 3_{10}-helix and π-bulge conformations relative to the pure α-helix concentration as the temperature increases. The $AmIII_3$ band in 50% methanol shows a shoulder at ~1258 cm^{-1} and another shoulder at ~1280 cm^{-1}, while the ~1240 cm^{-1} component is missing, indicating a lack of 3_{10}-helices. All helix spectra show an $AmIII_3$ band at ~1200 cm^{-1}, indicating turn structures (*26*). Calculated α-helix-like spectra in other alcohols

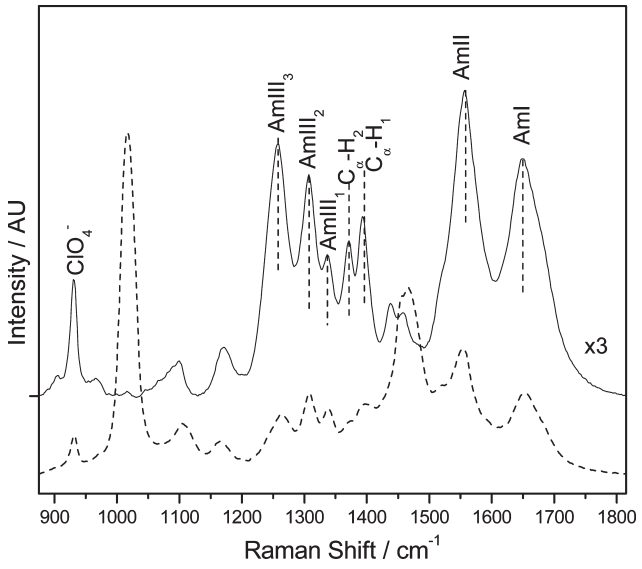

FIGURE 3: 204 nm excited UVRS of AP in pure water (—) and AP in 50% methanol (---) at 10 °C. The UVRS of AP in pure water was scaled to facilitate comparison.

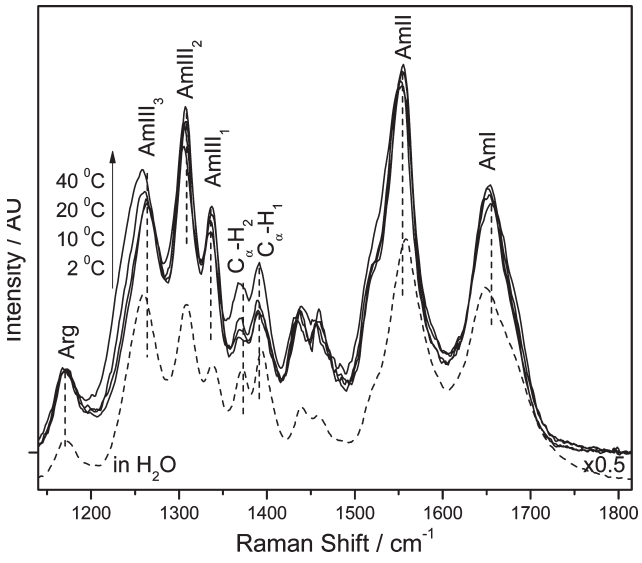

FIGURE 4: Temperature dependence of 204 nm excited UVRS of AP in 50% methanol (—) and UVRS of AP in pure water at 2 °C (---). The methanol contribution was subtracted. The UVRS of AP was scaled to facilitate comparison.

(not shown) are essentially identical to those in methanol, indicating similar ensembles of helical conformations.

We calculated the Gibbs free energy landscapes of AP (Figure 7) along the Ψ folding coordinate from the UVRR by using the methodology of Mikhonin et al. (*19*, *26*, *28*). The energy landscape (Figure 7) is bumpy within the α-helix-like basin. Within this basin, the pure α-helix conformation (Ψ ~ −45°) is always lowest in energy, followed by the π-bulge conformation. The 3_{10}-helix conformation (Ψ ~ −20°) lies at a slightly higher relative energy in pure water, but at much higher energies in alcohols. As the temperature increases, the α-helix basin Gibbs free energy in pure water increases, indicating that the α-helix is destabilized relative to the PPII-like conformation. The relative α-helix basin energies change very little with temperature in 50% alcohols. For all temperatures, the lowest α-helix Gibbs free

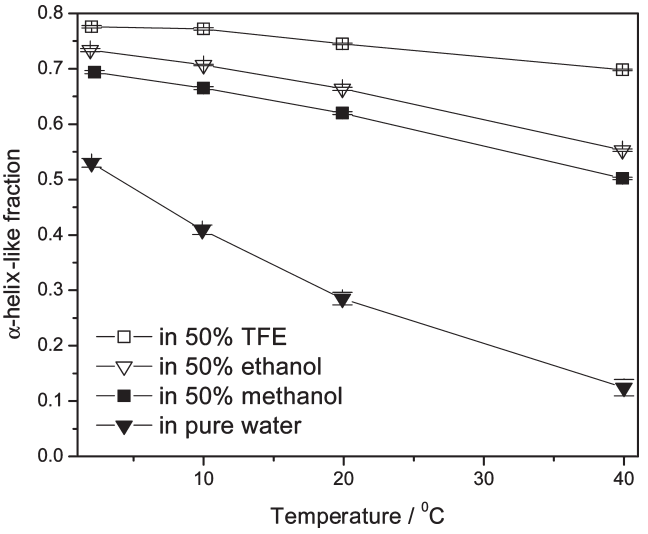

FIGURE 5: Raman-calculated AP α-helix-like fractions [primarily α-, 3_{10}-, and π-helix (bulge)] of AP in different solutions.

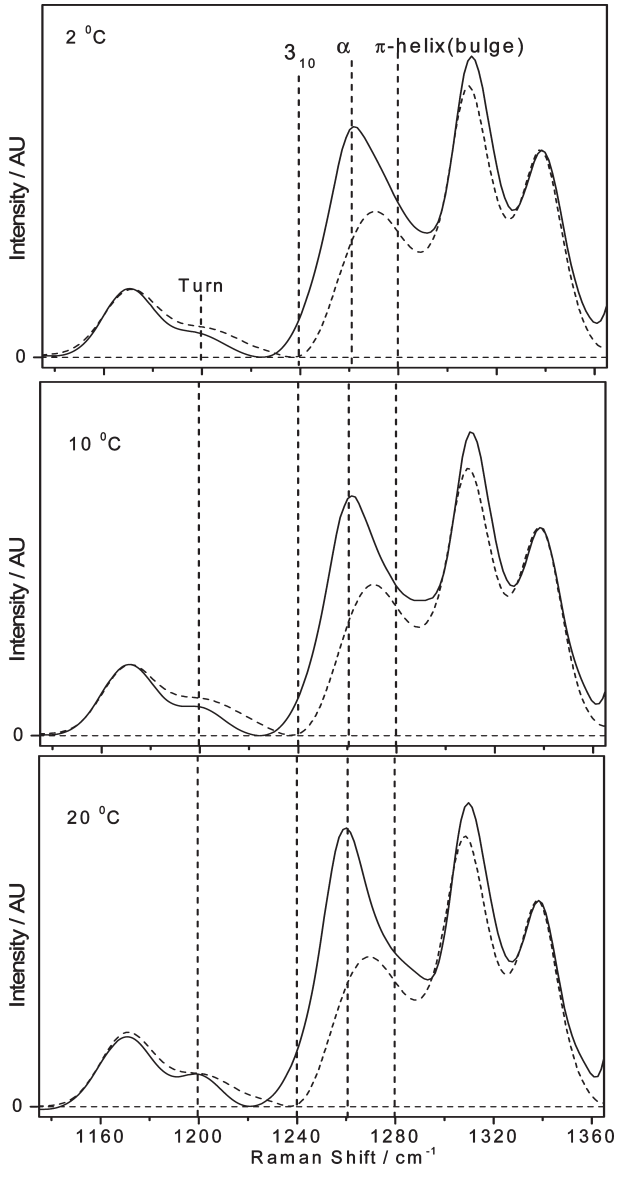

FIGURE 6: Calculated α-helix-like spectra of AP in pure water (—) and in 50% (v/v) methanol (---). Calculated α-helix-like difference spectra were normalized to the intensity of the AmIII$_1$ band.

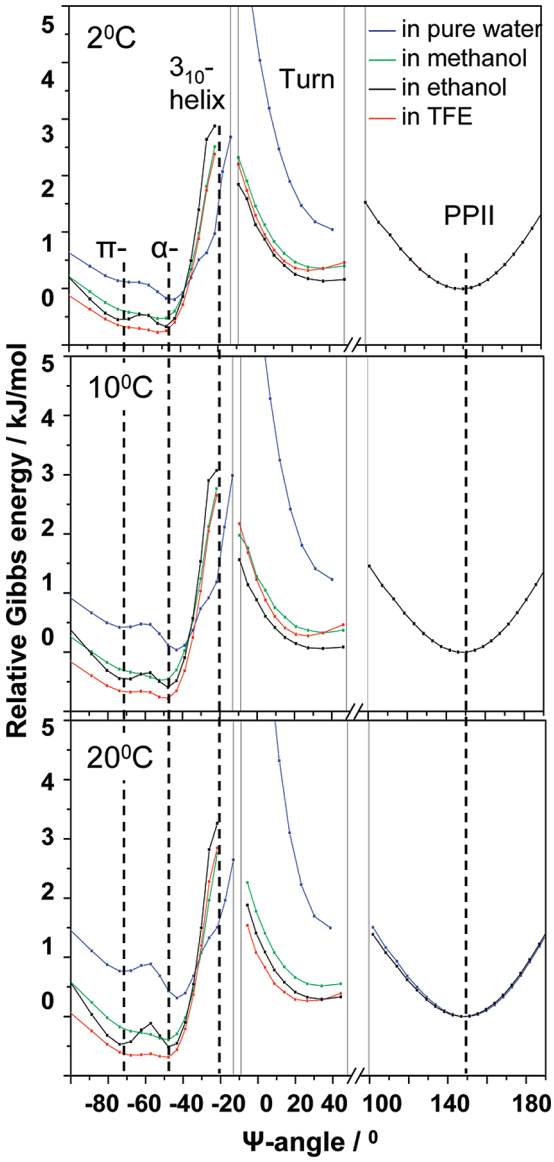

FIGURE 7: Calculated Gibbs free energy landscape of AP along the Ramachandran Ψ angle coordinate (blue line) in pure water, (green line) in 50% methanol, (black line) in 50% ethanol, and (red line) in 50% TFE. The PPII-like conformation is the reference state.

energies occur in 50% TFE, followed by ethanol, methanol, and finally pure water. The same trend is seen with the π-bulge energies. The alcohol-induced π-bulge energy decrease is larger than that of the α-helix. Turn conformations are stabilized by alcohols, consistent with previous observations that alcohols stabilize turns over PPII-like conformations (*29*). In contrast, 3_{10}-helix conformations are dramatically destabilized by alcohols.

DISCUSSION

Impact of Alcohols on the Gibbs Free Energies of Helices. Numerous studies indicate that alcohols induce α-helix formation in proportion to the bulkiness of their alcohol hydrocarbon group (*8*, *12*, *18*, *30*). This is confirmed by our UVRR results which show that the α-helix has the lowest Gibbs free energy in 50% TFE, followed by ethanol and methanol.

Alcohol molecules displace water in the peptide hydration shell which increases the hydrophobicity of the peptide−solvent interface, which should enhance intramolecular hydrogen bonding which should increase the α-helical content (*31*, *32*). Previous studies (*33*) indicate that 3_{10}-helices allow greater solvent access to the peptide bonds and thus are favored as the solvent hydrophilicity increases. In contrast, the α-helix and π-helix are more favored as the solvent hydrophobicity increases. It is also known that the 3_{10}-helix is favored in the peptide terminal regions where solvent exposure is greatest (*34*).

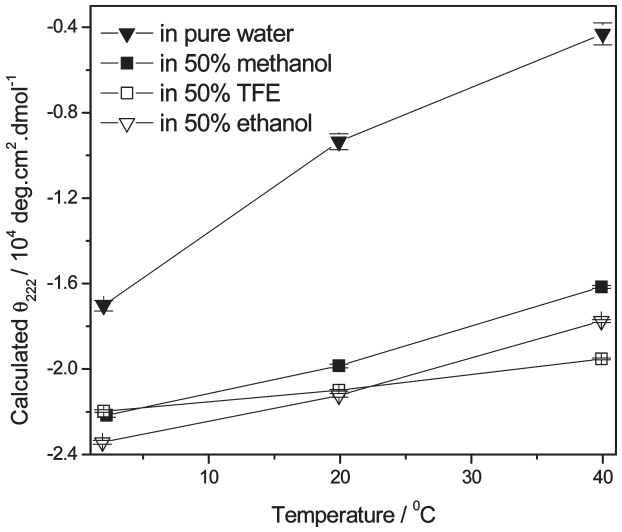

FIGURE 8: Calculated θ_{222} of AP in pure water and in 50% (v/v) alcohols.

TFE Induces Multihelix Segments. Our UVRR measurements that indicate that 50% TFE most stabilizes α-helix-like conformations appear to conflict with the CD measurements which show that 50% TFE does not significantly stabilize α-helical conformations more than 25% TFE. Previous studies (*22*, *35*−*37*) showed that UVRR-calculated α-helical conformation concentrations are higher than those calculated from CD (*36*) because the magnitude of the molar ellipticity per peptide bond (PB) decreases dramatically as the number of PBs within an α-helix decreases (*11*, *38*, *39*). In contrast, Raman is more linear; each peptide bond independently contributes to the Raman intensity (*36*, *40*) [except for the AmI band of the α-helical conformation where strong coupling between AmI vibrations exists (*41*)]. Thus, we can explain the spectroscopic results by proposing that TFE induces the most α-helical PBs but also breaks long helices into short helices (see Appendix I). Recent studies have showed that TFE binds strongly to peptides (*42*, *43*), while ethanol does not directly bind (*10*).

To quantify the dependence of the CD molar ellipticity per PB of an α-helix, θ_n, on the number of PBs within the helix, n, we fitted our experimental data to the empirical equation proposed by Chen et al. (*39*) (see Appendix II):

$$\theta_n = -34530\left(1-\frac{1.6}{n}\right)\ \text{deg cm}^2\ \text{dmol}^{-1} \qquad (1)$$

This allows us to relate the observed θ_{222} values to the UVRR-calculated helical fractions (see Appendix III). θ_{222} in 50% TFE calculated in Figure 8 is modeled to be less negative than that in 50% ethanol at low temperatures. [Calculated θ_{222} values are slightly more negative than those measured in Figure 2b because the $NaClO_4$ used as an internal standard in the UVRR measurements but not included in the CD measurements stabilizes the α-helix conformation (*27*).]

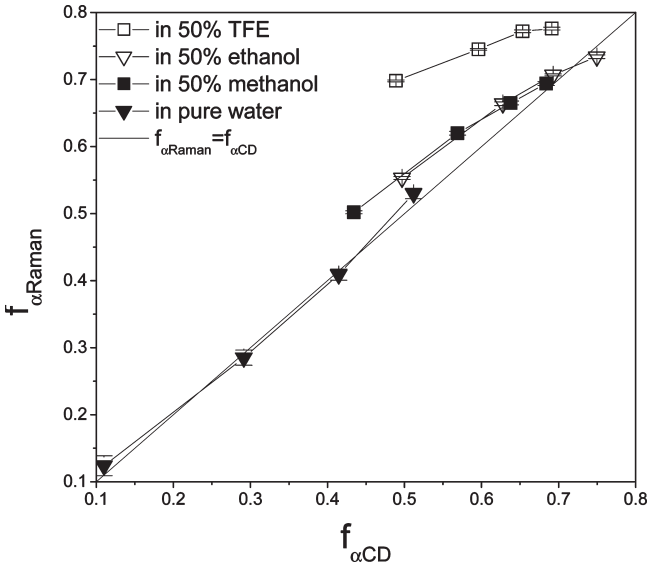

FIGURE 9: $f_{\alpha CD}$ vs $f_{\alpha Raman}$ of AP.

CONCLUSIONS

CD and UVRR measurements indicate that TFE most stabilizes the α-helix, followed by ethanol, methanol, and pure water. We determined the Gibbs free energy landscape from the UVRR spectra and found that the alcohol-induced π-bulge energy decrease is larger than that of the α-helix, while the 3_{10}-helix energy increases due to the alcohol-increased hydrophobicity. Turns are stabilized by alcohols as well. We also found that while TFE induces more α-helices, it favors multiple, shorter helical segments.

ACKNOWLEDGMENT

We thank Bhavya Sharma, Lu Ma, Zhenmin Hong, and David Punihaole for useful discussions.

APPENDIX I

TFE Induces More but Shorter Helices Than Other Alcohols. Suppose $\theta_\alpha(\theta_r)$ is the mean residue ellipticity for the pure α-helix [melted conformation(s)] [$\theta_\alpha = -26000$ deg cm^2 dmol^{-1}; $\theta_r = -3500$ deg cm^2 dmol^{-1} (*22*)], θ is the measured mean residue ellipticity of AP, and $f_{\alpha Raman}$ is the UVRR-calculated concentration of the α-helix-like conformation of AP. The CD α-helix fraction, $f_{\alpha CD}$, is calculated by (*22*)

$$f_{\alpha CD} = \frac{\theta - \theta_r}{\theta_\alpha - \theta_r} \tag{2}$$

$f_{\alpha Raman}$ and $f_{\alpha CD}$ are similar in pure water, 50% methanol, and 50% ethanol. A significant difference between $f_{\alpha Raman}$ and $f_{\alpha CD}$ is observed in 50% TFE which is likely due to the TFE-induced formation of short helices that show weakened CD signals (*36*). The proportionality between $f_{\alpha Raman}$ and $f_{\alpha CD}$ is decreased in TFE (Figure 9) relative to that in ethanol and methanol, indicating that TFE produces more but shorter helices. Given the energy cost of nucleating helix segments (*44*−*47*), it is unlikely that the 21-residue AP adopts more than two helix segments.

APPENDIX II

Quantify the Dependence of the CD Molar Ellipticity per PB of an α-Helix, θ_n, on the Number of PBs within the α-Helix, n. Suppose p_i is the probability of AP containing a single α-helix segment containing n_i α-helical PBs, $\bar{n}$ is the statistical average number of helical PBs, and $N = 20$, which is the total number of AP PBs. Thus

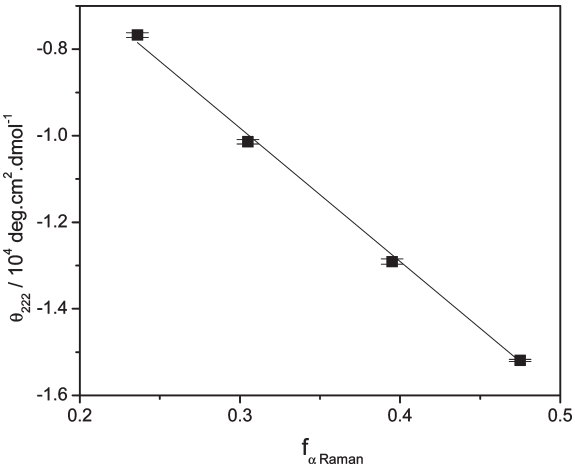

FIGURE 10: Linear fit of previously measured θ_{222} and $f_{\alpha Raman}$ values of AP in pure water (*27*).

$$\theta = \sum_i \left(\theta_{ni}\frac{n_i}{N} + \frac{N-n_i}{N}\theta_r\right)p_i \tag{3}$$

Substituting the empirical equation proposed by Chen et al. (*39*), $\theta_n = \theta_\infty(1 - k/n)$, into eq 3 yields

$$\theta = \sum_i \left[\theta_\infty\left(\frac{n_i}{N} - \frac{k}{N}\right) + \frac{N-n_i}{N}\theta_r\right]p_i$$

$$= \frac{\theta_\infty}{N}\sum_i n_i p_i - \frac{\theta_\infty k}{N}\sum_i p_i + \theta_r\sum_i p_i - \frac{\theta_r}{N}\sum_i n_i p_i$$

$$= \frac{\theta_\infty}{N}\bar{n} - \frac{\theta_\infty k}{N} + \theta_r - \frac{\theta_r}{N}\bar{n} \tag{4}$$

As the Raman intensity is more linear (*36*, *40*), the UVRR-calculated concentrations of α-helix-like conformations, $f_{\alpha Raman}$, more accurately monitor the fractions of α-helical PBs. Thus

$$f_{\alpha Raman} = \frac{\bar{n}}{N} \tag{5}$$

substituting eq 8 into eq , thus

$$\theta = (\theta_\infty - \theta_r)f_{\alpha Raman} + \left(\theta_r - \frac{k}{N}\theta_\infty\right) \tag{6}$$

We fit the experimental data to eq 6 (Figure 10) to obtain values of θ_n and n:

$$\theta_n = -34530\left(1 - \frac{1.6}{n}\right) \text{ deg cm}^2 \text{ dmol}^{-1} \tag{7}$$

APPENDIX III

Predicting CD Ellipticity from Raman-Calculated Concentrations of α-Helix-like Conformations.

Case 1. AP contains a single α-helix segment:

$$\theta = (\theta_\infty - \theta_r)f_{\alpha Raman} + \left(\theta_r - \frac{k}{N}\theta_\infty\right) \tag{8}$$

Case 2. AP contains two helix segments: p_i is the probability of AP containing one-helix segments of n_{i1} PBs and the second helix segment of n_{i2} PBs; $\bar{n}_1$ and $\bar{n}_2$ are the average numbers of helical

PBs in the first and second helix segments, respectively ($\bar{n}_1 + \bar{n}_2 = Nf_{\alpha\text{Raman}}$). Thus

$$\theta = \sum_i \left(\theta_{ni1}\frac{n_{i1}}{N} + \theta_{ni2}\frac{n_{i2}}{N} + \frac{N - n_{i1} - n_{i2}}{N}\theta_r \right) p_i$$

$$= \sum_i \left[\theta_\infty \left(\frac{n_{i1}}{N} - \frac{k}{N} \right) + \theta_\infty \left(\frac{n_{i2}}{N} - \frac{k}{N} \right) + \frac{N - n_{i1} - n_{i2}}{N}\theta_r \right] p_i$$

$$= \frac{\theta_\infty}{N}\sum_i (n_{i1} + n_{i2})p_i - 2\frac{k}{N}\sum_i p_i + \theta_r \sum_i p_i - \frac{\theta_r}{N}\sum_i (n_{i1} + n_{i2})p_i$$

$$= \frac{\theta_\infty}{N}\sum_i (n_i)p_i - 2\frac{k}{N}\sum_i p_i + \theta_r \sum_i p_i - \frac{\theta_r}{N}\sum_i (n_i)p_i$$

$$= \frac{\theta_\infty}{N}(\bar{n}_1 + \bar{n}_2) - 2\frac{k}{N} + \theta_r - \frac{\theta_r}{N}(\bar{n}_1 + \bar{n}_2)$$

$$= \theta_\infty f_{\alpha\text{Raman}} - 2\frac{k}{N} + \theta_r - \theta_r f_{\alpha\text{Raman}}$$

$$\therefore \theta = (\theta_\infty - \theta_r) f_{\alpha\text{Raman}} + \left(\theta_r - \frac{2k}{N}\theta_\infty \right) \quad (9)$$

We can then predict the observed CD ellipticity, θ, from $f_{\alpha\text{Raman}}$ in pure water, 50% methanol, and 50% ethanol by using eq 8 and in 50% TFE by using eq 7. The results are shown in Figure 8.

REFERENCES

1. Klibanov, A. M. (2001) Improving enzymes by using them in organic solvents. *Nature 409* (6817), 241–246.
2. Carrea, G., and Riva, S. (2000) Properties and synthetic applications of enzymes in organic solvents. *Angew. Chem., Int. Ed. 39* (13), 2226–2254.
3. Scharnagl, C., Reif, M., and Friedrich, J. (2005) Stability of proteins: Temperature, pressure and the role of the solvent. *Biochim. Biophys. Acta 1749* (2), 187–213.
4. Kony, D. B., Hunenberger, P. H., and van Gunsteren, W. F. (2007) Molecular dynamics simulations of the native and partially folded states of ubiquitin: Influence of methanol cosolvent, pH, and temperature on the protein structure and dynamics. *Protein Sci. 16* (6), 1101–1118.
5. Waterhous, D. V., and Johnson, W. C. (1994) Importance of Environment in Determining Secondary Structure in Proteins. *Biochemistry 33* (8), 2121–2128.
6. Roccatano, D. (2008) Computer simulations study of biomolecules in non-aqueous or cosolvent/water mixture solutions. *Curr. Protein Pept. Sci. 9* (4), 407–426.
7. Pace, C. N., Trevino, S., Prabhakaran, E., and Scholtz, J. M. (2004) Protein structure, stability and solubility in water and other solvents. *Philos. Trans. R. Soc. London, Ser. B 359* (1448), 1225–1234.
8. Hirota, N., Mizuno, K., and Goto, Y. (1998) Group additive contributions to the alcohol-induced α-helix formation of melittin: Implication for the mechanism of the alcohol effects on proteins. *J. Mol. Biol. 275* (2), 365–378.
9. Buck, M. (1998) Trifluoroethanol and colleagues: Cosolvents come of age. Recent studies with peptides and proteins. *Q. Rev. Biophys. 31* (3), 297–355.
10. Fioroni, M., Diaz, M. D., Burger, K., and Berger, S. (2002) Solvation phenomena of a tetrapeptide in water/trifluoroethanol and water/ethanol mixtures: A diffusion NMR, intermolecular NOE, and molecular dynamics study. *J. Am. Chem. Soc. 124* (26), 7737–7744.
11. Luo, P. Z., and Baldwin, R. L. (1997) Mechanism of helix induction by trifluoroethanol: A framework for extrapolating the helix-forming properties of peptides from trifluoroethanol/water mixtures back to water. *Biochemistry 36* (27), 8413–8421.
12. Kinoshita, M., Okamoto, Y., and Hirata, F. (2000) Peptide conformations in alcohol and water: Analyses by the reference interaction site model theory. *J. Am. Chem. Soc. 122* (12), 2773–2779.
13. Roccatano, D., Colombo, G., Fioroni, M., and Mark, A. E. (2002) Mechanism by which 2,2,2-trifluoroethanol/water mixtures stabilize secondary-structure formation in peptides: A molecular dynamics study. *Proc. Natl. Acad. Sci. U.S.A. 99* (19), 12179–12184.
14. Walgers, R., Lee, T. C., and Cammers-Goodwin, A. (1998) An Indirect Chaotropic Mechanism for the Stabilization of Helix Conformation of Peptides in Aqueous Trifluoroethanol and Hexafluoro-2-propanol. *J. Am. Chem. Soc. 120*, 5073–5079.
15. Reiersen, H., and Rees, A. R. (2000) Trifluoroethanol may form a solvent matrix for assisted hydrophobic interactions between peptide side chains. *Protein Eng. 13* (11), 739–743.
16. Roccatano, D., Fioroni, M., Zacharias, M., and Colombo, G. (2005) Effect of hexafluoroisopropanol alcohol on the structure of melittin: A molecular dynamics simulation study. *Protein Sci. 14* (10), 2582–2589.
17. Olivella, M., Deupi, X., Govaerts, C., and Pardo, L. (2002) Influence of the environment in the conformation of α-helices studied by protein database search and molecular dynamics simulations. *Biophys. J. 82* (6), 3207–3213.
18. Liu, H. L., and Hsu, C. M. (2003) The effects of solvent and temperature on the structural integrity of monomeric melittin by molecular dynamics simulations. *Chem. Phys. Lett. 375* (1−2), 119–125.
19. Bykov, S., Lednev, I., Ianoul, A., Mikhonin, A., Munro, C., and Asher, S. A. (2005) Steady-state and transient ultraviolet resonance Raman spectrometer for the 193−270 nm spectral region. *Appl. Spectrosc. 59* (12), 1541–1552.
20. Manning, M. C., and Woody, R. W. (1991) Theoretical CD studies of polypeptide helices: Examination of important electronic and geometric factors. *Biopolymers 31*, 569–586.
21. Asher, S., Mikhonin, A., and Bykov, S. (2004) UV Raman demonstrates that α-helical polyalanine peptides melt to polyproline II conformations. *J. Am. Chem. Soc. 126* (27), 8433–8440.
22. Lednev, I. K., Karnoup, A. S., Sparrow, M. C., and Asher, S. A. (1999) α-Helix peptide folding and unfolding activation barriers: A nanosecond UV resonance Raman study. *J. Am. Chem. Soc. 121* (35), 8074–8086.
23. Myshakina, N. S., Ahmed, Z., and Asher, S. A. (2008) Dependence of amide vibrations on hydrogen bonding. *J. Phys. Chem. B 112* (38), 11873–11877.
24. Wang, Y., Purrello, R., Jordan, T., and Spiro, T. G. (1991) UVRR spectroscopy of the peptide bond. 1. Amide S, a nonhelical structure marker, is a CαH bending mode. *J. Am. Chem. Soc. 113*, 6359–6368.
25. Mikhonin, A. V., Bykov, S. V., Myshakina, N. S., and Asher, S. A. (2006) Peptide secondary structure folding reaction coordinate: Correlation between UV Raman amide III frequency, ψ Ramachandran angle, and hydrogen bonding. *J. Phys. Chem. B 110* (4), 1928–1943.
26. Mikhonin, A. V., and Asher, S. A. (2006) Direct UV Raman monitoring of 3_{10}-helix and π-bulge premelting during α-helix unfolding. *J. Am. Chem. Soc. 128* (42), 13789–13795.
27. Xiong, K., Asciutto, E. K., Madura, J. D., and Asher, S. A. (2009) Salt Dependence of α-Helical Peptide Folding Energy Landscapes. *Biochemistry 48*, 10818–10826.
28. Ma, L., Ahmed, Z., Mikhonin, A. V., and Asher, S. A. (2007) UV resonance Raman measurements of poly-L-lysine's conformational energy landscapes: Dependence on perchlorate concentration and temperature. *J. Phys. Chem. B 111* (26), 7675–7680.
29. Liu, Z. G., Chen, K., Ng, A., Shi, Z. S., Woody, R. W., and Kallenbach, N. R. (2004) Solvent dependence of PII conformation in model alanine peptides. *J. Am. Chem. Soc. 126* (46), 15141–15150.
30. Dwyer, D. S. (1999) Molecular simulation of the effects of alcohols on peptide structure. *Biopolymers 49* (7), 635–645.
31. Deshpande, A., Nimsadkar, S., and Mande, S. C. (2005) Effect of alcohols on protein hydration: Crystallographic analysis of hen egg-white lysozyme in the presence of alcohols. *Acta Crystallogr. 61*, 1005–1008.
32. Starzyk, A., Barber-Armstrong, W., Sridharan, M., and Decatur, S. M. (2005) Spectroscopic evidence for backbone desolvation of helical peptides by 2,2,2-trifluoroethanol: An isotope-edited FTIR study. *Biochemistry 44* (1), 369–376.
33. Sorin, E. J., Rhee, Y. M., Shirts, M. R., and Pande, V. S. (2006) The solvation interface is a determining factor in peptide conformational preferences. *J. Mol. Biol. 356* (1), 248–256.
34. Millhauser, G. L., Stenland, C. J., Hanson, P., Bolin, K. A., and vandeVen, F. J. M. (1997) Estimating the relative populations of 3_{10}-helix and α-helix in Ala-rich peptides: A hydrogen exchange and high field NMR study. *J. Mol. Biol. 267* (4), 963–974.
35. Balakrishnan, G., Hu, Y., Bender, G. M., Getahun, Z., DeGrado, W. F., and Spiro, T. G. (2007) Enthalpic and entropic stages in α-helical peptide unfolding, from laser T-Jump/UV raman spectroscopy. *J. Am. Chem. Soc. 129* (42), 12801–12808.

36. Ozdemir, A., Lednev, I. K., and Asher, S. A. (2002) Comparison between UV Raman and circular dichroism detection of short α helices in Bombolitin III. *Biochemistry 41* (6), 1893–1896.
37. Ianoul, A., Mikhonin, A., Lednev, I. K., and Asher, S. A. (2002) UV resonance Raman study of the spatial dependence of α-helix unfolding. *J. Phys. Chem. A 106* (14), 3621–3624.
38. Woddy, R. W. (1996) Circular Dichroism and the Conformational Analysis of Biomolecules, pp 25−68, Plenum Press, New York.
39. Chen, Y.-H., Yang, J. T., and Chau, K. H. (1974) Determination of the helix and β-form of proteins in aqueous solution by circular dichroism. *Biochemistry 13*, 3350–3359.
40. Mikhonin, A. V., and Asher, S. A. (2005) Uncoupled peptide bond vibrations in α-helical and polyproline II conformations of polyalanine peptides. *J. Phys. Chem. B 109* (7), 3047–3052.
41. Myshakina, N. S., and Asher, S. A. (2007) Peptide bond vibrational coupling. *J. Phys. Chem. B 111* (16), 4271–4279.
42. Gerig, J. T. (2004) Structure and solvation of melittin in 1,1,1,3,3,3-hexafluoro-2-propanol/water. *Biophys. J. 86* (5), 3166–3175.
43. Diaz, M. D., and Berger, S. (2001) Preferential solvation of a tetrapeptide by trifluoroethanol as studied by intermolecular NOE. *Magn. Reson. Chem. 39* (7), 369–373.
44. Hong, Q., and Schellman, J. A. (1992) Helix-Coil Theories: A Comparative-Study for Finite Length Polypeptides. *J. Phys. Chem. 96* (10), 3987–3994.
45. Doig, A. J. (2002) Recent advances in helix-coil theory. *Biophys. Chem. 101*, 281–293.
46. Yang, J. X., Zhao, K., Gong, Y. X., Vologodskii, A., and Kallenbach, N. R. (1998) α-Helix nucleation constant in copolypeptides of alanine and ornithine or lysine. *J. Am. Chem. Soc. 120* (41), 10646–10652.
47. Scholtz, J. M., Qian, H., York, E. J., Stewart, J. M., and Baldwin, R. L. (1991) Parameters of helix-coil transition theory for alanine-based peptides of varying chain length in water. *Biopolymers 31*, 1463–1470.